ELSEVIER

Journal of Orthopaedic Research 19 (2001) 977–984

Journal of Orthopaedic Research

www.elsevier.com/locate/orthres

Contribution of disc degeneration to osteophyte formation in the cervical spine: a biomechanical investigation

Srirangam Kumaresan [a], Narayan Yoganandan [a], Frank A. Pintar [a,*], Dennis J. Maiman [a], Vijay K. Goel [b]

[a] *Department of Veterans Affairs, Medical College of Wisconsin, VA Medical Center Research 151, 5000 West National Avenue Medical Center, Milwaukee, WI 53295, USA*

[b] *Department of Biomedical Engineering and Orthopedics, Iowa Spine Research Center, University of Iowa, Iowa City, IA 53295, USA*

Received 27 November 2000; accepted 2 December 2000

Abstract

Cervical spine disorders such as spondylotic radiculopathy and myelopathy are often related to osteophyte formation. Bone remodeling experimental–analytical studies have correlated biomechanical responses such as stress and strain energy density to the formation of bony outgrowth. Using these responses of the spinal components, the present study was conducted to investigate the basis for the occurrence of disc-related pathological conditions. An anatomically accurate and validated intact finite element model of the C4-C5-C6 cervical spine was used to simulate progressive disc degeneration at the C5-C6 level. Slight degeneration included an alteration of material properties of the nucleus pulposus representing the dehydration process. Moderate degeneration included an alteration of fiber content and material properties of the anulus fibrosus representing the disintegrated nature of the anulus in addition to dehydrated nucleus. Severe degeneration included decrease in the intervertebral disc height with dehydrated nucleus and disintegrated anulus. The intact and three degenerated models were exercised under compression, and the overall force–displacement response, local segmental stiffness, anulus fiber strain, disc bulge, anulus stress, load shared by the disc and facet joints, pressure in the disc, facet and uncovertebral joints, and strain energy density and stress in the vertebral cortex were determined. The overall stiffness (C4-C6) increased with the severity of degeneration. The segmental stiffness at the degenerated level (C5-C6) increased with the severity of degeneration. Intervertebral disc bulge and anulus stress and strain decreased at the degenerated level. The strain energy density and stress in vertebral cortex increased adjacent to the degenerated disc. Specifically, the anterior region of the cortex responded with a higher increase in these responses. The increased strain energy density and stress in the vertebral cortex over time may induce the remodeling process according to Wolff's law, leading to the formation of osteophytes. © 2001 Orthopaedic Research Society. Published by Elsevier Science Ltd. All rights reserved.

Introduction

Formation of osteophytes adjacent to a degenerated disc is often implicated to cause cervical spondylotic myelopathy and radiculopathy [6,19]. From a biomechanical perspective, the intervertebral disc is the connecting medium between the vertebrae for the transmission of external force in a physiological environment, and it facilitates spinal mobility [3,23]. During the degeneration process, the disc undergoes progressive structural changes in the form of desiccation of the nucleus pulposus and disintegration of the anulus fibrosus resulting in decreased disc height [2,8]. These structural changes affect the overall and internal biomechanical responses. Dehydration of the nucleus increases the compression stiffness (overall response) and reduces disc fiber strain (internal response) at the degenerated level as determined from a finite element model of the lumbar motion segments [14]. In addition, variations in stress or strain in the spinal structure may explain the structural changes that occur during the degeneration process. Consequently, an examination of changes in the internal response of the spine structure due to disc degeneration will provide a better understanding of the clinical problem, i.e., formation of osteophytes.

Nathan conducted a detailed anatomical study of cervical spines and attributed the presence of osteophytes adjacent to degenerated discs to higher pressure transmitted through the vertebral disc [22]. In another anatomical study by Shore, the osteophyte formation was

* Corresponding author. Tel.: +1-414-384-2000 ext. 46933; fax: +1-414-384-3493.

E-mail address: fpintar@mcw.edu (F.A. Pintar).

0736-0266/01/$ - see front matter © 2001 Orthopaedic Research Society. Published by Elsevier Science Ltd. All rights reserved.
PII: S0736-0266(01)00010-9

again attributed to higher stress [28]. Radiographic examinations of patients have shown osteophytes in the presence of reduced disc height [6]. Theories of bone remodeling phenomena have also shown that bony outgrowth stems from higher stress or strain energy density [1,4,12]. All these studies have suggested that higher vertebral stress or strain energy density adjacent to the degenerated disc may be responsible for pathological conditions such as the formation of osteophytes. Based on the above considerations, our working hypothesis was that degenerative changes in the cervical intervertebral disc can lead to structural changes in adjacent bony components due to higher internal response(s).

Experimental and mathematical models are used to study the biomechanics of the spine [7,30,31]. To investigate the biomechanical effects due to degeneration of a spinal component (e.g., intervertebral disc), experimental models such as in vitro human cadavers are not particularly useful. Although a gross dissection can be made after experimentation, the assessment of disc degeneration is not quantitative. Disc degeneration cannot be accurately assessed using radiographs or computed tomography (CT) scans without specific enhancement techniques such as discography. In contrast, mathematical finite element models are well suited to study such phenomena as appropriate material properties can be assigned representing the various stages in the degeneration process [16,29]. In addition, it is possible to isolate or individually investigate the effects of degeneration of a particular disc component (e.g., nucleus dehydration) on internal biomechanical responses such as anulus fiber strain. Consequently, the finite element modeling approach was used to quantify the overall and internal responses of the cervical spine during progressive degenerative changes in the intervertebral disc and to investigate the plausible biomechanical reasons for the formation of osteophytes during disc degeneration.

Methods

A three-dimensional, anatomically accurate, geometrically and materially nonlinear, and experimentally validated adult finite element model of the human cervical spine (C4-C5-C6) was used (Fig. 1). A detailed description of model development and validation has been presented previously [15,29]. The geometrical details of bony and soft tissue components were obtained from 1.0 mm CT images (coronal and sagittal) and cryomicrotome anatomical sections of a human cadaver specimen. The specimen preparation and subsequent imaging procedure incorporated the natural lordosis of the cervical spine. Since the finite element model accurately simulated the geometrical details of the cervical spine, the lordotic curvature was maintained [17,29]. The finite element model included all the critical components of the spine: cortical and cancellous bone, endplates, spinous processes, laminae, pedicle and transverse processes of vertebrae; anulus fibrosus and nucleus pulposus of the intervertebral disc; synovial fluid and surrounding membranes of uncovertebral joints; synovial fluid, articular cartilage, synovial membranes of the facet joints; and the anterior longitudinal, posterior longitudinal, interspinous and capsular ligaments, and ligamentum flavum.

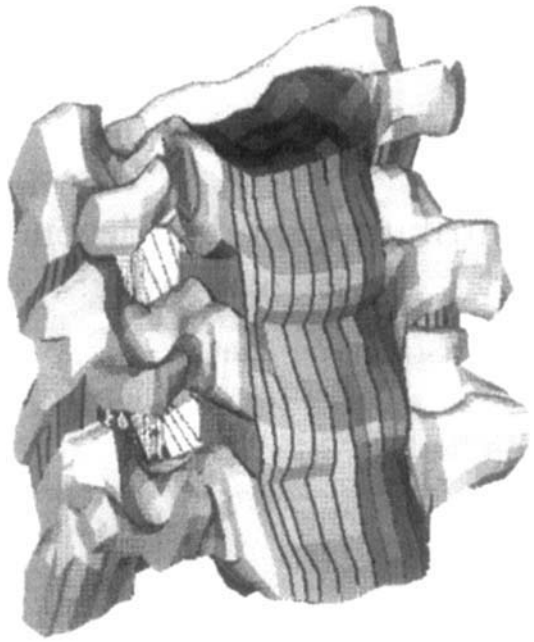

Fig. 1. The finite element model of a human cervical spine (C4–C5–C6).

The cortical bone, cancellous bone, endplates, and posterior elements of vertebrae and articular cartilage of facet joints were simulated using eight-noded isoparametric solid elements. The anulus fibrosus of the intervertebral disc was defined using a fiber-reinforced approach. The collagen fibers were modeled using rebar elements, and the ground substance matrix was defined using solid elements. The rebar elements were defined to carry only tensile forces. The nucleus pulposus of the intervertebral disc and the synovial fluid in the facet and uncovertebral joints were defined using incompressible fluid elements. Synovial membranes enclosing uncovertebral and facet joints were modeled using membrane elements. All ligaments (anterior longitudinal, posterior longitudinal, interspinous, capsular, and ligamentum flavum) were modeled using nonlinear tension-active cable elements. The finite element model consisted of 12,712 elements and 15,577 nodes. Material property values for each spinal component (Table 1) were adopted from the literature [17]. The finite element model was exercised using the principles of geometric and material nonlinearities. The computed force–displacement and moment-rotation responses and localized strain data in the vertebral body and bilateral facet masses were validated with experimental results [17,24,26]; these data are given for completeness (Fig. 2). To the best of our knowledge, this is the only model that has been validated to this extent with experimental data. This validated intact finite element model (C4-C5-C6) was used to simulate progressive degenerative changes in the intervertebral disc at the caudal level (C5-C6) leaving the cephalad level (C4-C5) intact.

Degenerative changes in the intervertebral disc were classified as slight, moderate, and severe based on structural changes reported in the literature [19,21]. These three progressive grades of disc degenerative conditions were simulated at the caudal (C5-C6) level in the intact finite element model. Grade 1 (slight degeneration) was represented by alteration of material properties to represent in vivo dehydration process of the nucleus pulposus. To simulate this condition, the incompressible fluid elements of nucleus pulposus and uncovertebral joint of the intervertebral disc were replaced with isoparametric solid elements. Typically, the process of disc degeneration initiates in the form of dehydration in the nucleus pulposus and uncovertebral joints [19]. During this process, the fluid content in the nucleus region reduces and transforms to a granular semi-solid. To simulate this dehydrated condition in the finite element model, hydrostatic incompressible fluid elements were replaced with stiffer solid elements. The elastic modulus of simulated nucleus was two times the elastic modulus of anulus ground substance in the intact model [14]. Grade 2 (moderate degeneration) included Grade 1 changes and added alteration of the fiber

Table 1
Finite element model details

Components	Element type	Elastic modulus (MPa)	Poisson's ratio
Cortex	Solid	12000.0	0.30
Cancellous core	Solid	100.0	0.20
Endplate	Solid	600.0	0.30
Posterior elements	Solid	3500.0	0.25
Disc anulus ground substance	Solid	4.7	0.45
Disc anulus fibers	Rebar	500.0	0.30
Disc nucleus pulposus	Fluid	1666.7[a]	
Facet articular cartilages	Solid	10.4	0.40
Facet synovial fluid	Fluid	1666.7[a]	
Facet synovial membrane	Membrane	12.0	0.40
Uncovertebral synovial fluid	Fluid	1666.7[a]	
Uncovertebral synovial membrane	Membrane	12.0	0.40
Ligaments	Cable (defined using nonlinear force–deflection response)		

Anterior longitudinal		Posterior longitudinal		Interspinous		Ligamentum flavum		Capsular	
Deflection (mm)	Force (N)	Deflection (mm)	Force (N)	Deflection (mm)	Force (N)	Deflection (mm)	Force (N)	Deflection (mm)	Force (N)
1.4	35.5	1.0	29.0	1.3	16.9	1.9	45.9	1.8	53.6
2.7	64.9	2.0	51.4	2.7	24.4	3.7	82.4	3.9	87.9
4.1	89.7	3.0	71.3	4.0	29.5	5.6	119.6	5.8	109.4
5.4	108.6	4.0	85.8	5.4	32.9	7.5	133.7	7.7	125.8
6.8	119.6	5.0	94.7	6.7	34.9	9.4	147.2	9.7	134.8

[a] Bulk modulus (MPa).

content and material properties of the anulus fibrosus representing the disintegrated nature of the anulus. The elastic modulus of anulus ground substance was assigned two times the value of anulus ground substance in the intact model, and the anulus fiber volume was reduced by 25% from the value of the intact model [8]. Grade 3 (severe degeneration) included Grades 1 and 2 changes and added a decrease in the intervertebral disc height. The disc height was reduced by 25% to obtain the Grade 3 model representing the more advanced stage of degeneration [6].

The intact and three degenerated (slight, moderate and severe) cervical spine models were exercised under compression (80 N). The boundary condition was simulated by fixing the inferior surface of the C6 vertebra with all degrees of freedom constrained. The external load was applied to the nodes of the superior surface of the C4 vertebra with the superior–inferior translation degree of freedom unconstrained. Rotations were also allowed. The resulting force–displacement response was computed. The overall stiffness was obtained between C4 and C6 levels. The segmental stiffnesses between C4 and C5 levels (intact) and between C5 and C6 levels (degenerated) were determined. The maximum values of the anulus fiber strain, anterior and posterior disc bulges, and anulus ground substance stress (von Mises) in the C4-C5 and C5-C6 intervertebral discs were obtained. The loads shared by the disc and facet joints and pressure in the disc, facet and uncovertebral joints were computed. The load transmitted through the intervertebral disc was computed by adding the resultant forces along the nodes connecting the disc and vertebral body. The load resisted by the facet joint was determined by adding the resultant forces along the nodes connecting the inferior articular cartilage and facet bone. The maximum value of strain energy density and principal stress (minimum) in the anterior and posterior cortex of the C4, C5, and C6 vertebrae were obtained.

Results

The overall force–displacement response of the three degenerated spines shifted toward ordinate (stiffer) compared to the normal spine (Fig. 3). The increase in overall stiffness of degenerated spinal columns increased with the severity of degeneration, i.e., lowest in slightly degenerated model, and increased progressively. The segmental stiffnesses also changed with the severity of degeneration (Table 2). However, the segmental stiffness increased considerably (57%) at the degenerated level (C5-C6). Similarly, the responses of the intervertebral disc and facet joints varied considerably at the degenerated level (Table 2). At the intact level, the load shared by the disc and facet joints and the pressure in the disc, facet and uncovertebral joints showed minimal variation. In contrast, at the degenerated level, the load transmitted through the facet joint and facet pressure decreased, and the load through the disc joint increased. In addition, the disc bulges, anulus stress, and anulus fiber strain of the degenerated disc decreased with the severity of degeneration (Table 2). While the anterior and posterior disc bulges and anulus fiber strain decreased progressively, the anterior and posterior anulus stress decreased initially and increased subsequently. In contrast to the decrease in anulus fiber strain and intervertebral disc bulge with the severity of degeneration, responses of the vertebral cortex adjacent to the degenerated level increased (Figs. 4 and 5). The strain energy density and stress in the C5 and C6 vertebral cortex increased. Specifically, the anterior region of the cortex responded with a higher increase in these responses than the posterior region (Fig. 6).

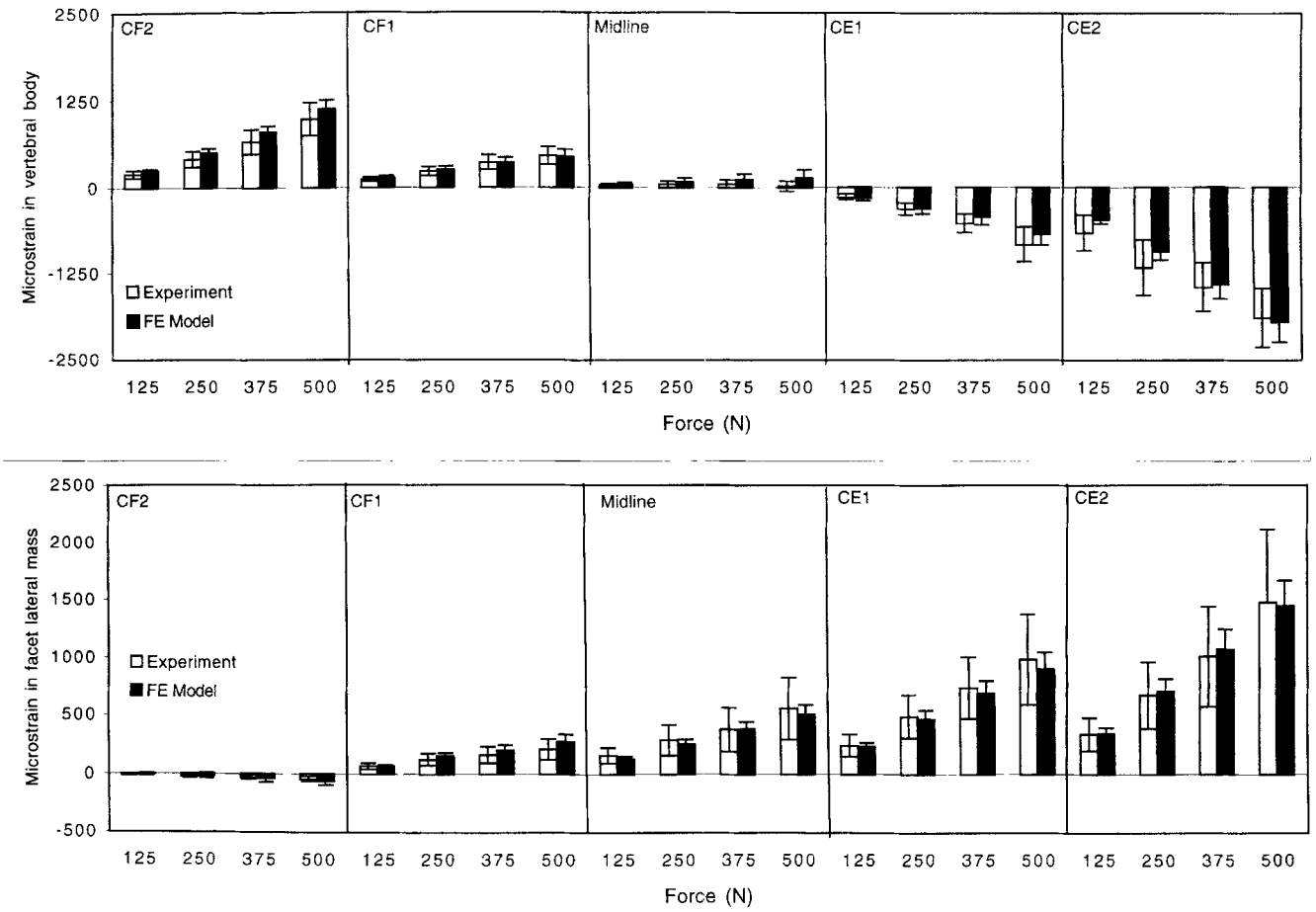

Fig. 2. Comparison of tissue level responses (strain data in the anterior region of interest in the vertebral body (top) and bilateral facet masses (bottom)) with experimental results [24]. CF2 and CF1 refer to compression–flexion load at 2 and 1 cm from the posterior longitudinal ligament, respectively. Midline refers to compression at the posterior longitudinal ligament. CE1 and CE2 refer to compression–extension load at 1 and 2 cm from the posterior longitudinal ligament, respectively.

Discussion

The study hypothesized that physical property changes in degenerative discs lead to osteophyte formation. While not fully testable, an anatomically accurate, three-dimensional, nonlinear finite element model of the cervical spine was used to support this hypothesis. Results indicated that the strain energy density and stress (internal responses) in the bony vertebra adjacent to the degenerated disc increased. The increase in these responses is related to the severity of degeneration. The increase in the vertebral stress matches with the findings of Shirazi et al. and Kurowski et al. [18,27]. Shirazi et al. [27] varied the nucleus volume of the intervertebral disc to represent the degenerated condition. The loss of nucleus volume resulted in an increase in the vertebral cortex stress. Kurowski et al. [18] simulated the loss of hydrostatic behavior of the nucleus in the intervertebral disc and found that stresses in the vertebral components increased. The increase in overall stiffness due to disc degeneration found in this investigation coincides with the observation of loss of mobility or restricted motion reported in clinical and anatomical studies [5]. The increase in overall stiffness also matches with the results of an experimental study using the cervical spine motion

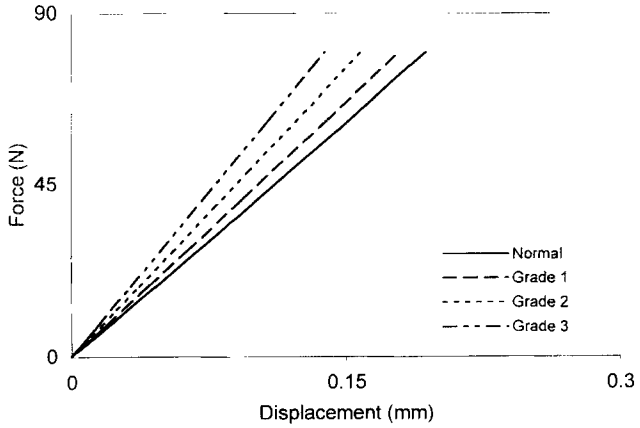

Fig. 3. Overall force–displacement response (C4 vertebra with respect to C6 vertebra) under pure compression. Grade 1: Slight degeneration. Grade 2: Moderate degeneration. Grade 3: Severe degeneration.

Table 2
Biomechanical parameters at the C4-C5 and C5-C6 intervertebral levels

Parameters		Normal	Grade 1	Grade 2	Grade 3
Load sharing (%)					
	C4-C5 Disc	61.5	61.8	61.5	61.6
	C4-C5 Facet	38.5	38.2	38.5	38.4
	C5-C6 Disc	69.3	70.3	70.9	70.9
	C5-C6 Facet	30.7	29.7	29.1	29.1
Facet pressure (MPa)					
	C4-C5	0.191	0.189	0.191	0.189
	C5-C6	0.128	0.126	0.121	0.110
Disc pressure (MPa)					
	C4-C5	0.250	0.250	0.248	0.248
	C5-C6	0.272	–	–	–
Uncovertebral joint pressure (MPa)					
	C4-C5	0.243	0.243	0.239	0.237
	C5-C6	0.241	–	–	–
Intersegmental stiffness (N/mm)					
	C4-C5	1027.0	925.9	949.0	956.9
	C5-C6	689.7	859.3	1082.5	1459.9
Disc bulge (mm)					
	C4-C5 – Anterior	0.103	0.101	0.095	0.093
	C4-C5 – Posterior	0.128	0.126	0.127	0.126
	C5–C6 – Anterior	0.149	0.085	0.058	0.048
	C5-C6 – Posterior	0.124	0.073	0.047	0.034
Anulus stress (MPa)					
	C4-C5 – Anterior	0.567	0.569	0.539	0.522
	C4-C5 – Posterior	0.508	0.509	0.484	0.469
	C5-C6 – Anterior	0.576	0.234	0.346	0.370
	C5-C6 – Posterior	0.310	0.144	0.212	0.221
Anulus fiber strain (%)					
	C4-C5	0.346	0.346	0.336	0.341
	C5-C6	0.436	0.294	0.208	0.150

segment intact units [20] in which the overall stiffness of the intact unit increased with disc degeneration. The localized effects of degeneration such as decreases in the anterior and posterior bulges of the degenerated disc follow the results of decreased disc bulge at the degenerated level compared to the intact level reported by Goel and associates [14].

The present study is an initial step toward a better understanding of biomechanics of cervical spine degeneration. The model includes ligamentous components of the cervical spine. It is known that the inclusion of muscles renders the model more realistic. Consequently, results of this study should be considered as a first approximation of the spinal response. The model includes a two-motion segment (C4-C5-C6) of the human cervical spine. The extension of the model to include superior and inferior levels will provide an estimation of the entire cervical column behavior. We are advancing our studies to include these levels. The present results are applicable only to axial load. This loading mode was chosen because the cervical spine is being constantly loaded by the head mass. The selected load magnitude is in close agreement with a previous study by Goel, et al. wherein a compressive load of 73.6 N was applied in their cervical spine finite element model [10]. In addition, this load magnitude falls within the range of compressive load (47–276 N) calculated by measuring the intradiscal pressure and disc area [11,25]. It should be noted that the present study included only the degenerative changes in the disc component although changes occur in the remaining components of the spine. This was done to highlight the effect of degenerative changes in the disc on overall and local internal responses and to study the structural changes in the spine associated with disc degeneration. In addition, although

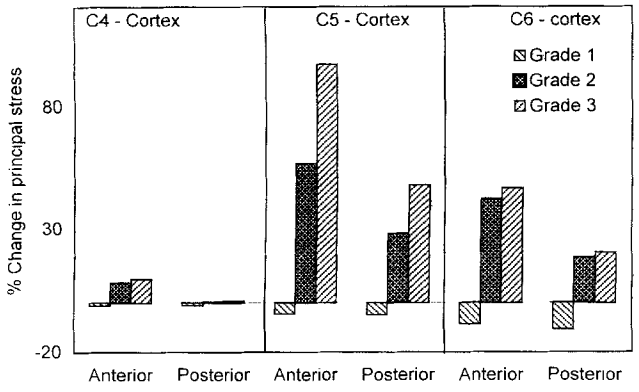

Fig. 4. Percentage change in the principal stress in the anterior and posterior cortices of C4, C5 and C6 vertebrae. Grade 1: Slight degeneration. Grade 2: Moderate degeneration. Grade 3: Severe degeneration.

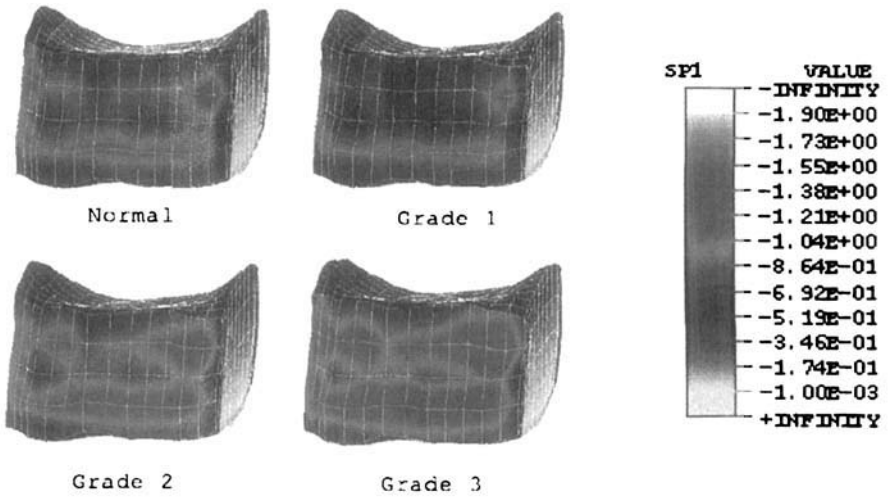

Fig. 5. Principal stress distribution in the anterior region of the C5 vertebral cortex. The stress distribution increased with the severity of degeneration.

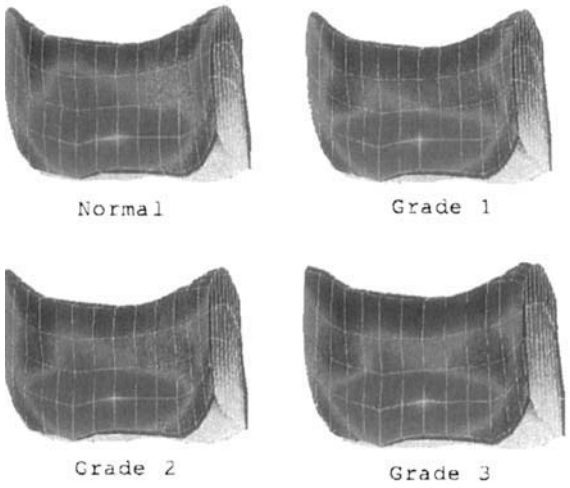

Fig. 6. Principal stress distribution in the posterior region of the C5 vertebral cortex. The stress distribution did not show considerable increase with the severity of degeneration as seen in the anterior region.

the model was validated with experimental data with regard to parameters such as force–deflection curve and strains in the vertebral body and facets, it did not encompass the entire range of conditions represented in the study, i.e., varying degrees of disc degeneration. Furthermore, material property changes used in the input for representing the various degrees of degeneration were obtained from the finite element modeling literature (see Methods). This is because of a paucity of such data from experimental studies on disc tissues of the cervical spine. Other studies that may ultimately affect the accuracy of the model prediction are disc swelling, tissue pre-stress (pre-strain), and other physiologic constraints such as vertebral motion and alterations in trabecular architecture, which can occur in association with disc degeneration.

The results indicated that overall stiffness of the degenerated spinal columns increased with the severity of degeneration. The increase in stiffness was lowest with slight degeneration and highest with severe degeneration. This suggests that the biomechanical behavior of the spinal column is related directly to the severity level of disc degeneration. Similarly, the segmental stiffness increased at the degenerated level indicating that the effect of degeneration is localized. This is further evident from the variation in load sharing by the disc and facet joint at the degenerated level. While the load transmitted through the facet joint decreased, the load through the disc joint increased. It is well known that facet and disc joints are the primary medium of load transmission in the cervical spine under a compressive loading mode. The findings of a decrease in the facet load and an associated increase in the disc load indicated that the facet and disc joints supplement each other to maintain the structural equilibrium. However, the change in load sharing between disc and facet joints may not directly indicate the biomechanical consequences of disc degeneration. Perhaps the alteration of the pathway along which the load is transmitted through the disc joint better explains the effect of disc degeneration. The change in the load pathway along the disc joint can be studied by examining the internal responses of the degenerated disc and bony vertebrae adjacent to the disc. The present results indicated that the internal responses (strain energy density and stress) of vertebral components increased with degeneration which may explain the structural changes in adjacent bony components associated with disc degeneration.

It is known that the bone tissue responds to chronic changes in stresses and strain according to Wolff's law. Brown et al. conducted a combined experimental-finite element modeling study to select the specific mechanical

parameters responsible for initiating the adaptive responses of bone using an animal model [1]. The authors compared 24 parameters with the quantified adaptive experimental responses. Results indicated that the strain energy density, tensile principal stress and strain, and longitudinal shear stress are probable parameters associated with the initiation of the remodeling process. Goel et al. demonstrated that the strain energy density in the vertebral cortex and cancellous bone induce the remodeling process in the form of external shape optimization and internal variations in elastic moduli, respectively [9]. Keller et al. also demonstrated that the regional material properties (bone mineral density, elastic moduli, ultimate stress and strain, and stiffness) of vertebral bodies directly correlate with the degenerative conditions of the intervertebral disc [13].

It is clear from these studies that the bony vertebrae respond to variations in strain energy density and stress which may induce a remodeling process and lead to the formation of osteophytes. Consequently, the model responses induced by the degeneration process were directly compared with a previous study [9]. The computed increase in maximum strain energy density in the vertebral cortex (7.8–9.4E−4 J/mm^3) between the intact and severely degenerated models is in close agreement with the reported strain energy density (8.84E−4 J/mm^3) for external remodeling to optimize the vertebral body shape [9]. The authors conducted a bone remodeling adaptive study based on strain energy density as the feedback control variable to analyze the shape of the verteberal bodies. In this study, homeostatic strain energy density (8.84E−4 J/mm^3) distribution throughout the structure was used as a criterion for the remodeling process. To further correlate the findings of the present study, region-specific strain energy density and stress responses were examined. The higher increases in strain energy density and stress were noted in the anterior region of the vertebral cortex compared to the posterior region. This finding may be correlated to the presence of anterior osteophytes in the cervical vertebral column [22]. The above explanations may provide biomechanical reasons for the formation of osteophytes observed in anatomical, radiographic, and mathematical remodeling studies. Further research is required, however, to determine if these specific changes in stress/strain are the direct cause.

In summary, the biomechanical effects of progressive degenerative changes in the intervertebral disc were quantified using a three-dimensional, nonlinear, anatomically accurate and experimentally validated finite element model of the human cervical spine (C4-C5-C6). The overall stiffness (C4-C6) of the spine increased with increasing severity of degeneration. The increase in segmental stiffness was considerably higher at the degenerated level (C5-C6). Intervertebral disc bulge, and anulus stress and strain decreased at the degenerated level. The strain energy density and stress of the vertebral cortex increased adjacent to the degenerated disc. Specifically, the anterior region of the cortex responded with higher increases in these parameters. These observations underscore the localized effects of disc degenerative changes on the biomechanics of the cervical spine. The increased strain energy density and stress in the vertebral cortex may induce remodeling process over a period of time according to Wolff's law leading to the formation of osteophytes.

Acknowledgements

This study was supported by the Department of Veterans Affairs Medical Research.

References

[1] Brown T, Pederson D, Gray M, Brand R, Rubin C. Toward an identification of mechanical parameters initiating periosteal remodeling: a combined experimental and analytic approach. J Biomech 1990;23(9):893–905.
[2] Buckwalter JA. Aging and degeneration of the human intervertebral disc. Spine 1995;20(11):1307–14.
[3] Ching R, Tencer A, Anderson P, Daly C. Comparison of residual stability in thoracolumbar spine fractures using neutral zone measurements. J Orthop Res 1995;13(4):533–41.
[4] Cowin SC. Bone mechanics. Boca Ranton, FL: CRC Press; 1989.
[5] Dai L. Disc degeneration and cervical instability: correlation of magnetic resonance imaging with radiography. Spine 1998; 23(16):1734–8.
[6] Friedenberg Z, Miller W. Degenerative disc disease of the cervical spine. J Bone Jt Surg 1963;45-A(6):1171–8.
[7] Garfin S, Lee T, Roux R, Silva F, Ballock R, Botte M, Katz M, Woo S. Structural behavior of the halo orthosis pin–bone interface: biomechanical evaluation of standard and newly designed stainless steel halo fixation pins. Spine 1986;11(10):977–81.
[8] Ghosh P. Biology of the intervertebral disc. Boca Raton, FL: CRC Press; 1988.
[9] Goel V, Ramirez S, Kong W, Gilbertson L. Cancellous bone young's modulus variation within the vertebral body of a ligamentous lumbar spine: application of bone adaptive remodeling concepts. J Biomech Eng 1995;117:266–71.
[10] Goel VK, Clausen JD. Prediction of load sharing among spinal components of a C5-C6 motion segment using the finite element approach. Spine 1998;23(6):684–91.
[11] Hattori S, Oda H, Kawai S. Cervical intradiscal pressure in movements and traction of the cervical spine. Z Orthop 1981; 119:568.
[12] Huiskes R, Weinana H, Grootenboor H, Dalstra M, Fudala B, Slooff T. Toward an identification of mechanical parameters initiating periosteal remodeling: a combined experimental and analytic approach. J Biomech 1987;20:1135–50.
[13] Keller T, Hansson T, Abram A, Spengler D, Panjabi M. Regional variations in the compressive properties of lumbar vertebral trabeculae: effects of disc degeneration. Spine 1989;14:1012–9.
[14] Kim YE, Goel VK, Weinstein JN, Lim TH. Effects of disc degeneration of one level on the adjacent level in axial mode. Spine 1991;16:331–5.

[15] Kumaresan S, Yoganandan N, Pintar F, Voo L, Cusick J, Larson S. Finite element modeling of cervical laminectomy with graded facetectomy. J Spinal Disord 1997;10(1):40–7.
[16] Kumaresan S, Yoganandan N, Pintar FA. Finite element analysis of the cervical spine: a material property sensitivity study. Clin Biomech 1999;14(1):41–53.
[17] Kumaresan S, Yoganandan N, Pintar FA, Maiman DJ. Finite element modeling of the lower cervical spine: Role of intervertebral disc under axial and eccentric loads. Med Eng Phys, in press.
[18] Kurowski P, Kubo A. The relationship of degeneration of the intervertebral disc to mechanical loading conditions on lumbar vertebrae. Spine 1986;11(7):726–31.
[19] Lestini W, Wiesel S. The pathogenesis of cervical spondylosis. Clin Orthop Rel Res 1989;239:69–93.
[20] Moroney S. Mechanical properties and muscle force analyses of the lower cervical spine. Doctoral Dissertation. Chicago: University of Illinois; 1984.
[21] Natarajan RN, Ke JH, Andersson BJ. A model to study the disc degeneration process. Spine 1994;19(3):259–65.
[22] Nathan H. Osteophytes of the vertebral column. J Bone Jt Surg 1962;44(2):243–68.
[23] Patwardhan A, Havey R, Meade K, Lee B, Dunlap B. A follower load increases the load-carrying capacity of the lumbar spine in compression. Spine 1999;4(10):1003–9.
[24] Pintar FA, Yoganandan N, Pesigan M, Reinartz JM, Sances Jr A, Cusick JF. Cervical vertebral strain measurements under axial and eccentric loading. J Biomech Eng 1995;117:474–8.
[25] Pooni JS, Hukins DW, Harris PF, Hilton RC, Davies KE. Comparison of the structure of human intervertebral discs in the cervical, thoracic and lumbar regions of the spine. Surg Radiol Anat 1986;8:175–82.
[26] Shea M, Edwards WT, White AA, III, Hayes WC. Variations of stiffness and strength along the human cervical spine. J Biomech 1991;24(2):95–107.
[27] Shirazi-Adl SA. Finite element simulation of changes in the fluid content of human lumbar discs: mechanical and clinical implications. Spine 1992;17(2):206–12.
[28] Shore L. Polyspondylitis marginalis osteophytica. Brit J Surg 1935; 22:850–63.
[29] Yoganandan N, Kumaresan S, Voo L, Pintar F. Finite element model of the human lower cervical spine. J Biomech Eng 1997; 119(1):87–92.
[30] Yoganandan N, Pintar FA, editors. Frontiers in Whiplash Trauma: clinical and biomechanical. Amsterdam, The Netherlands: IOS Press; 2000. p. 590.
[31] Yoganandan N, Pintar FA, Larson SJ, Sances Jr A, editors. Frontiers in head and neck trauma: clinical and biomechanical. Amsterdam; The Netherlands: IOS Press; 1998. p. 743.